

Model of coherent passive mode locking in a two-section ring-cavity laserAnton Pakhomov ^{1,*} and Rostislav Arkhipov ^{1,2}¹*St. Petersburg State University, St. Petersburg 199034, Russia*²*Ioffe Institute, St. Petersburg 194021, Russia*

(Received 17 December 2023; accepted 6 February 2024; published 18 March 2024)

We propose a simple and convenient analytical model for the description of coherent passive mode locking in a two-section ring-cavity laser based on the generalized area theorem for the coherent pulse propagation in a resonant medium with inhomogeneous line broadening. This model is applied to theoretically analyze the possible regimes of the spatiotemporal dynamics of such a laser together with their stability properties. We examined the laser dynamics, when varying the energy and phase relaxation times in the media, the gain and absorption rate in the respective laser sections, as well as the ratio of the transition dipole moments of the absorber and gain media. As the result, the stability of the coherent mode locking as well as the large flexibility of the arising laser behavior were shown in wide parameter ranges.

DOI: [10.1103/PhysRevA.109.033519](https://doi.org/10.1103/PhysRevA.109.033519)**I. INTRODUCTION**

Ultrafast lasers represent the most convenient source of ultrashort pulses up to the few-cycle duration for most applications in optical data transmission or the control of high-speed physical and chemical processes [1–3]. The most widely used method for the ultrashort pulse generation in lasers is passive mode locking (PML) [4,5]. This method is based on the use of a passive nonlinear intracavity component (saturable absorber) to ensure the in-phase interference of multiple longitudinal cavity modes, resulting in a regular output pulse series. Passively mode-locked lasers are routinely used nowadays for the generation of trains of femtosecond light pulses. For example, in recent papers [6–11] the possibility of sub-100-fs pulse generation in semiconductor disk lasers and vertical-external-cavity surface-emitting lasers was demonstrated. Moreover, self-starting few-picosecond pulse generation by means of the passive mode locking has also been recently achieved in the terahertz range in a semiconductor laser with multilayer-graphene saturable absorbers [12].

At the same time, the passively mode-locked lasers completely rely on the incoherent interaction of the produced pulses with the intracavity media. This means that the obtained pulse duration largely exceeds the dephasing time of the active media T_2 so that the phase matching between multiple resonant centers in the medium induced by the driving field rapidly vanishes within the pulse duration. As the result, such passively mode-locked lasers exhibit certain principal restrictions on their output parameters. First, the duration of the produced mode-locked pulses is strongly limited from below by the value of the phase relaxation time T_2 in the active medium [1,3]. Besides that, incoherent pulse-matter interaction leads to inevitable energy losses in the laser

absorber section and only partial energy extraction from the gain section.

The natural way to overcome these principal limitations implies the use of the coherent light-matter interaction. In such a case the pulse duration must be well below the dephasing time of the active media T_2 and the phase matching between resonant centers in the medium caused by the pulse field is now preserved over the pulse duration. The respective approach for the mode locking in lasers is called coherent mode locking (CML) and has been actively studied over the past few decades [13–25]. Sometimes this approach is also called self-induced transparency mode locking, since in its standard formulation the generated pulse can propagate in the laser absorber in the self-induced transparency regime, i.e., fully inverting the absorber medium at the pulse leading edge and then fully restoring it to the noninverted state at the trailing edge [13–15].

Since coherently mode-locked lasers are based on the coherent interaction of the generated pulses with the laser media, such lasers are free of any limitations typical for standard passively mode-locked ones. Specifically, by means of the coherent mode-locking, pulses much shorter in duration than the dephasing time T_2 are produced [13–25]. Moreover, it was even shown that the generation of regular single-cycle pulse series can be realized in certain laser geometries [16,17,21].

Although the CML has been mainly studied theoretically so far, several experimental works have also been done. In particular, the CML regime was successfully experimentally demonstrated with the gaseous active media, though with only absorber section operating under the coherent-interaction conditions [24,25]. At the same time, it should be noted that the coherent pulse-matter interaction as well as the self-induced transparency phenomena were experimentally achieved in many resonant media so far, including solid-state ones [26–31].

In the treatment of standard (“incoherent”) passive mode locking in laser systems the coherent effects are commonly

*antpakhom@gmail.com

ignored. However, the ongoing transition to more compact laser sources and shorter pulse durations urges the need to take coherent effects in mode-locked laser systems into account [20,21,28,32–34]. For example, experimental evidence of the significance of coherent effects was found in Ti:sapphire laser systems generating femtosecond pulses [34], in quantum cascade lasers [28] and in gas lasers [33]. In this case, conventional passive mode-locking theories based on incoherent approaches [35–40] are already invalid and novel theoretical approaches should be developed.

The theoretical studies of the CML lasers were previously mainly based on the numerical solution of the laser Maxwell-Bloch equations. There is a number of analytical tools developed for the analysis of the passively mode-locked lasers based on either partial-differential equations [41,42] or delay differential equations [40,43–46]. However, all these models are specifically derived on the assumption of the incoherent pulse-matter interaction and either completely neglect coherent effects or treat them as small perturbations [47,48] and thus cannot be applied for modeling of CML lasers.

Another possible way is given by the area theorem, which provides a convenient analytical description of the coherent pulse propagation in an inhomogeneously broadened two-level resonant medium [49–52]. The area theorem is valid as long as the Rabi frequency stays well below the laser carrier frequency, i.e., until the so-called carrier-wave Rabi flopping regime starts to arise [53,54]. Several extensions of the standard area theorem were later derived, e.g., for the field evolution in a single-mode ring cavity [55,56], a single-mode Fabry-Perot cavity [57], dense medium [58], or pulse propagation in a single-mode waveguide [59].

The area theorem in its standard form was earlier used for the rough analysis of the dynamics of CML lasers in Refs. [19,20,23]. However, both the standard area theorem and its later extensions are barely suitable for the description of the CML laser operation, since they were derived just for a single pulse pass through a resonant medium. In real CML lasers, however, the produced pulse circulates inside the cavity and the medium excitation left after each pulse passage does not make it to fully relax until the pulse enters the medium again after a full round trip inside the cavity. Therefore such medium-mediated self-action of the produced pulse has to be properly taken into account.

The respective generalization of the standard area theorem suitable for the pulse area evolution on the pulse propagation in a ring cavity was recently derived in Ref. [60]. Still this generalized area theorem has not yet been applied for the analytical description of the CML laser dynamics. In Ref. [60] it was only used for a single-section ring-cavity laser with the gain section only. At the same time the two-section laser configuration with the gain and absorber section respectively in general provides much greater variety of the arising spatiotemporal dynamics. It should be also noted that the comprehensive analysis of the CML laser dynamics in dependence on the media and cavity parameters has not been performed so far.

In this paper, we develop a model for the dynamics of a coherently mode-locked two-section laser with a ring cavity. Suggested model stems from the generalized area theorem derived in Ref. [60] and allows us to analyze the possible

generation regimes in a general two-section CML laser. We investigate the dependence of the steady values of the pulse area, induced medium polarization, and population inversion in both laser sections on the control parameters. Specifically, we vary the values of the relaxation times in the intracavity media, the gain and absorption rate in the respective sections, as well as the ratio of the transition dipole moments in the absorber and gain media.

The paper is organized as follows. In Sec. II we work out our mathematical model based on the generalized area theorem for a ring-cavity configuration of a two-section CML laser. Besides that, we determine the required ranges of the system parameters to be examined. In Sec. III we use the derived model and provide the detailed analysis of the CML laser dynamics and the arising steady-state solutions vs the variations of the control parameters. Finally, paper summary and concluding remarks are given in Sec. IV.

II. MODEL

For the following analysis we will make use of the area theorem, which deals with the so-called pulse area, defined as [49–51]:

$$\Phi(z) = \frac{d_{12}}{\hbar} \int_{-\infty}^{+\infty} E(z, t) dt, \quad (1)$$

where d_{12} is the dipole moment of the medium resonant transition, $E(z, t)$ is the slowly varying envelope of the electric field in the propagating pulse, and \hbar is the reduced Planck constant.

We assume the following inequalities to hold for the duration of the produced pulse τ , the coherence relaxation time T_2 in the resonant medium (equal to the inversed width of the homogeneously broadened line), and the inversed width of the inhomogeneously broadened line Ω :

$$\Omega^{-1} \ll \tau \ll T_2. \quad (2)$$

Under these conditions the spatial evolution of the pulse area in a resonant medium is provided by the general relation [51,52]:

$$\frac{d\Phi}{dz} = F_{\text{prior}} + F_{\text{induced}}, \quad (3)$$

where the first term:

$$F_{\text{prior}} = \frac{2\pi\omega_{12}d_{12}}{n_{\text{ph}}\hbar c} \int_{-\infty}^{+\infty} g(\Delta) d\Delta \int_0^\tau P_0(\Delta, z) e^{i\Delta t} dt', \quad (4)$$

describes the contributions of the medium polarization present prior the pulse arrival, and the second term,

$$F_{\text{induced}} = \frac{2\pi\omega_{12}d_{12}^3}{n_{\text{ph}}\hbar^2 c} \int_{-\infty}^{+\infty} g(\Delta) d\Delta \int_0^\tau dt' \times \int_0^{t'} E(z, t'') N(\Delta, t'', z) e^{i\Delta(t'-t'')} dt'', \quad (5)$$

provides the contribution of the pulse-induced nonlinear response of the resonant medium. Here the following parameters are used: $P_0 = P(\Delta, z, t = 0)$ is the slowly varying envelope of the medium polarization at the time point of the pulse arrival, ω_{12} is the medium's resonant frequency,

N_0 is the volume concentration of two-level resonant centers, $N(\Delta, t, z)$ is the population inversion in the resonant medium per unit volume, $g(\Delta)$ is the normalized-to-unity spectral function of inhomogeneously broadened dipole transitions in the medium, Δ is the frequency detuning from the center of the inhomogeneously broadened line, and n_{ph} is the phase refractive index of the host medium at the pulse carrier frequency ω_{12} . It is assumed in Eqs. (4) and (5) that the propagating pulse at the spatial point z begins at $t = 0$ and is completely gone by the time point $t = \tau$, so that τ represents the overall pulse duration. Thereby the time-domain integration in Eqs. (4) and (5) is performed over the whole duration of the propagating pulse.

It is well known that in a medium with strongly inhomogeneous line broadening the volume polarization left after an excitation pulse decays on the timescale $\sim \Omega^{-1}$ due to the so-called free polarization decay [51], i.e., the dephasing between oscillating dipoles with different resonant frequencies:

$$\int_{-\infty}^{+\infty} P_0(\Delta, z, t_0) e^{i\Delta(t-t_0)} g(\Delta) d\Delta \rightarrow 0, \text{ if } t - t_0 \gg \Omega^{-1}. \quad (6)$$

Due to presumed relations Eq. (2) this characteristic time of the volume polarization decay due to dephasing in our case is even shorter than the pulse duration. As the time separation in between consecutive pulses should be larger than the pulse duration, we find that the induced medium polarization fully vanishes by the arrival of the next considered pulse. Now comparing Eqs. (4) and (6) one can see that inequalities Eq. (2) lead to vanishing of the first term in the right-hand side of the evolution equation Eq. (3):

$$F_{\text{prior}} = 0. \quad (7)$$

The second term in the right-hand side of Eq. (3) under the conditions Eq. (2) gets reduced as follows [51,52,58]:

$$F_{\text{induced}} \rightarrow \frac{2\pi^2 \omega_{12} g(0) d_{12}}{n_{\text{ph}} \hbar c} \cdot [P(0, z, t = \tau) - P(0, z, t = 0)]. \quad (8)$$

Using the expression for $P(0, z, t = \tau)$ derived in Ref. [60] and combining Eqs. (3), (7), and (8) we end up with:

$$\frac{d\Phi}{dz} = \alpha \left[N(0, z, t = 0) \sin \Phi(z) - \frac{2P(0, z, t = 0)}{d_{12}} \sin^2 \frac{\Phi(z)}{2} \right], \quad (9)$$

with the coupling factor:

$$\alpha = \frac{2\pi^2 \omega_{12} d_{12}^2 g(0)}{n_{\text{ph}} \hbar c}.$$

Having obtained the evolution equation for the pulse area $\Phi(z)$, we now turn to a pulse circulating inside a ring cavity in the coherent light-matter interaction conditions. Let us denote the spatial dependence of the pulse area at the n th round trip as $\Phi_n(z)$ and in-resonance components (i.e., with zero frequency detuning $\Delta = 0$) of the population inversion and the induced medium polarization after n full round trips just before the pulse arrives to the spatial point z at the $(n + 1)$ -th round

trip as $N_{a/g,n}(z)$ and $P_{a/g,n}(z)$. Here and in the following the subscript ‘‘a’’ refers to the absorber section and the subscript ‘‘g’’ refers to the gain section.

We assume that, although the macroscopic medium polarization rapidly vanishes after the pulse passage due to the free polarization decay, the medium excitation for the resonant centers at the pulse carrier frequency (i.e., ones with zero frequency detuning from the pulse central frequency) does not yet relax until the next pulse arrival after a full round trip in the cavity. The explicit equations for the evolution of the induced medium polarization and the population inversion against both the longitudinal coordinate z and the number of iteration n (i.e., the number of round trips) were derived in Ref. [60].

Then putting these equations together with the Eq. (9) for the dynamics of the pulse area we get the model for the unidirectional pulse circulation inside a ring cavity in the following form:

$$\begin{aligned} \frac{d\Phi_{a/g,n+1}(z)}{dz} &= \alpha_{a/g} \left[N_{a/g,n}(z) \sin \Phi_{a/g,n+1}(z) - \frac{2P_{a/g,n}(z)}{d_{12,a/g}} \sin^2 \frac{\Phi_{a/g,n+1}(z)}{2} \right], \\ \text{where } 0 \leq z \leq L_{\text{cav}}, \\ N_{a/g,n+1}(z) &= \left[N_{a/g,n}(z) \cos \Phi_{a/g,n+1}(z) - \frac{P_{a/g,n}(z)}{d_{12,a/g}} \sin \Phi_{a/g,n+1}(z) \right] \\ &\cdot e^{-T_n/T_{1,a/g}} + N_{0,a/g} (1 - e^{-T_n/T_{1,a/g}}), \\ P_{a/g,n+1}(z) &= [P_{a/g,n}(z) \cos \Phi_{a/g,n+1}(z) + d_{12,a/g} \cdot N_{a/g,n}(z) \sin \Phi_{a/g,n+1}(z)] e^{-T_n/T_{2,a/g}}, \\ \text{where } 0 \leq z \leq L_{\text{absorber/gain}}, \end{aligned} \quad (10)$$

with the cavity length L_{cav} ; the length of the absorber section L_{absorber} ; the length of the gain section L_{gain} ; the cavity round-trip time T_n ; the dephasing time $T_{2,a/g}$ and the lifetime of the excited level $T_{1,a/g}$ in the absorber and gain, respectively; the transition dipole moments in the absorber and gain $d_{12,a/g}$; the coupling factors $\alpha_{a/g}$; the pumping level in the gain medium $N_{0,g} > 0$; and the equilibrium population inversion in the absorber (absorption rate) $N_{0,a} < 0$.

Equations for the evolution of the induced medium polarization and the population inversion in Eq. (10) were derived in Ref. [60] by the direct integration of the two-level Bloch equations with zero frequency detuning $\Delta = 0$ at each spatial point z over a single full round trip in the ring laser cavity. For this we made use of the relation Eq. (2) between the pulse duration and the medium relaxation times. First, over the pulse duration the relaxation terms were neglected, what gives the well-known harmonic solution for the medium quantities [the very first expressions in parenthesis in the right-hand sides of equations for $N_{a/g,n+1}(z)$ and $P_{a/g,n+1}(z)$ in Eq. (10)]. Afterwards, as the generated pulse at each spatial point z is gone, the two-level Bloch equations are simply integrated over the time interval $T_n - \tau \approx T_n$ assuming no electric field. The respective solution for this case simply yields the exponential decay of the medium polarization to its initial zero value with

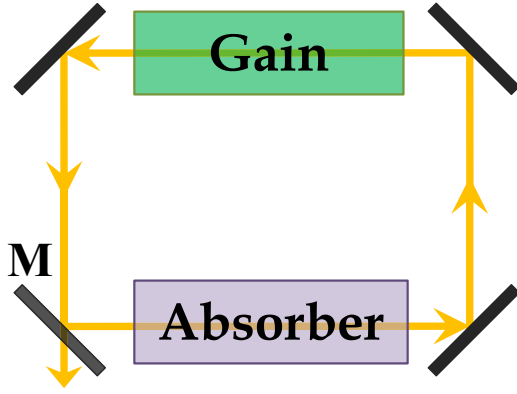


FIG. 1. The scheme of the considered two-section ring-cavity laser with the output mirror M ; the arrows show the direction of the unidirectional field propagation.

the decay time T_2 and the exponential decay of the population inversion to its stable value $N_{0,a/g}$ with the decay time T_1 [the exponential factors in the right-hand sides of equations for $N_{a/g,n+1}(z)$ and $P_{a/g,n+1}(z)$ in Eq. (10) and the second term in the right-hand side of the equation for $N_{a/g,n+1}(z)$].

For a two-section laser Eq. (10) has to be supplemented with the relations between the output and input values of the pulse area in both sections. Namely, for a laser arrangement

$$\tan \left[\frac{\Phi_{a/g,n+1}(z)}{2} \right] = \tan \left[\frac{\Phi_{a/g,n+1}(0)}{2} \right] \cdot e^{\alpha_{a/g} \int_0^z N_{a/g,n}(z') dz'} \cdot \left\{ 1 + \frac{\alpha_{a/g}}{d_{12,a/g}} \tan \left[\frac{\Phi_{a/g,n+1}(0)}{2} \right] \cdot \int_0^z P_{a/g,n}(z') e^{\alpha_{a/g} \int_0^{z'} N_{a/g,n}(z'') dz''} dz' \right\}^{-1}, \quad 0 \leq z \leq L_{\text{absorber/gain}}. \quad (15)$$

Using the obtained laser model [Eqs. (10) and (15)], one can readily obtain the solutions $\Phi_{n+1}(z)$, $P_{a/g,n+1}(z)$, and $N_{a/g,n+1}(z)$ corresponding to the $(n+1)$ -th round trip, provided that the functions for the n th round trip $\Phi_n(z)$, $P_{a/g,n}(z)$, and $N_{a/g,n}(z)$ are already known. We fix the initial values of the functions to be

$$\begin{aligned} \Phi_0(z) &= 0, & 0 \leq z \leq L_{\text{cav}}, \\ P_{a,0}(z) &= 0, & 0 \leq z \leq L_{\text{absorber}}, \\ N_{a,0}(z) &= N_{0,a}, & 0 \leq z \leq L_{\text{absorber}}, \\ P_{g,0}(z) &= 0, & 0 \leq z \leq L_{\text{gain}}, \\ N_{g,0}(z) &= N_{0,g}, & 0 \leq z \leq L_{\text{gain}}. \end{aligned} \quad (16)$$

Thus we end up with the initial-value problem for the system of equations composed of the direct equations for the pulse area $\Phi_{n+1}(z)$ Eq. (15) and four direct equations for the medium quantities $P_{a/g,n+1}(z)$ and $N_{a/g,n+1}(z)$ in Eq. (10), which can be easily solved.

The derived model could be, however, simplified even further, if assuming the induced medium polarizations and the population inversions to negligibly vary across the whole length of the respective laser sections. This means that one ignores the spatial dependencies of the medium quantities and approximates them as roughly constant in space, i.e.,

like the one sketched in Fig. 1, the initial pulse area in the absorber is

$$\Phi_{a,n+1}(0) = r m_d \Phi_{g,n}(L_{\text{gain}}), \quad (11)$$

and the initial pulse area in the gain is

$$\Phi_{g,n+1}(0) = \Phi_{a,n}(L_{\text{absorber}})/m_d, \quad (12)$$

where r is the amplitude reflection coefficient of the output cavity mirror and we have explicitly introduced the new variable m_d for the ratio of the transition dipole moments in both media:

$$m_d = \frac{d_{12,a}}{d_{12,g}}. \quad (13)$$

It should be noted here that in the limit $T_1, T_2 \ll T_{\text{rt}}$ the population inversion and the induced medium polarization fully relax to their equilibrium values $N_{a/g,n}(z) = N_{0,a/g}$ and $P_{a/g,n}(z) = 0$ during the round-trip time. The equation for the pulse area in Eq. (10) in this simplest case reduces to the classic one [50–52]:

$$\frac{d\Phi_{n+1}(z)}{dz} = \alpha_{a/g} N_{0,a/g} \sin \Phi_{n+1}(z), \quad 0 \leq z \leq L_{\text{cav}}. \quad (14)$$

Fortunately, the only differential equation for the pulse area $\Phi_{n+1}(z)$ in the model Eq. (10) does permit the general analytical solution as:

$P_{a/g,n}(z) \approx \text{const}$ and $N_{a/g,n}(z) \approx \text{const}$. In this case we can simply calculate the integrals over the spatial variable z in Eq. (15), which yields:

$$\begin{aligned} \tan \left[\frac{\Phi_{a/g,n+1}(z)}{2} \right] &= \tan \left[\frac{\Phi_{a/g,n+1}(0)}{2} \right] e^{\alpha_{a/g} z N_{a/g,n}} \\ &\cdot \left\{ 1 + \frac{P_{a/g,n}}{d_{12,a/g} N_{a/g,n}} \tan \left[\frac{\Phi_{a/g,n+1}(0)}{2} \right] \right. \\ &\cdot \left. \left(e^{\alpha_{a/g} z N_{a/g,n}} - 1 \right) \right\}^{-1}, \\ &0 \leq z \leq L_{\text{absorber/gain}}, \end{aligned} \quad (17)$$

with the same relations at the boundaries of each laser section:

$$\begin{aligned} \Phi_{a,n+1}(0) &= r m_d \Phi_{g,n}(L_{\text{gain}}), \\ \Phi_{g,n+1}(0) &= \Phi_{a,n}(L_{\text{absorber}})/m_d. \end{aligned}$$

When fixing $z = L_{\text{absorber}}$ or $z = L_{\text{gain}}$ in the respective sections, the obtained Eq. (17) together with the equations for the medium evolution in Eq. (10) (here one can take the pulse area, for instance, equal to the arithmetic mean of its values at the boundaries of each section) form a simple mapping for the values of the pulse area and the medium quantities expressed through their values at the previous round trip. Therefore

one can equally use both the general model Eq. (10), especially for calculating the spatially extended functions, and the reduced mapping Eq. (17), which is particularly suitable for analyzing the parameter dependencies of the stable solutions.

Let us now specify the parameter ranges, where one should solve the system Eq. (10). First, for small-enough gain in the laser no lasing is to appear. To be more specific, one can easily see that the growth rate for the small values of the pulse area in the gain section is given as $e^{\alpha_g L_g N_{0,g}}$, while the respective decay rate in the absorber section is $e^{\alpha_a L_a N_{0,a}} < 1$. The lasing can start, as long as the net amplification of a small field perturbation exceeds the losses on the reflection at the output mirror M . Therefore we end up with the following expression for the lasing threshold:

$$r e^{\alpha_g L_g N_{0,g} + \alpha_a L_a N_{0,a}} = 1. \quad (18)$$

Hence, only for those values of the parameters r , $\alpha_g L_g N_{0,g}$, and $\alpha_a L_a N_{0,a}$, which give the left-hand side of Eq. (18) greater than 1, should the CML generation be investigated.

Next, it is important to determine the values of the coherence relaxation rate in the medium T_2 , where the CML regime can exist. As multiple studies of the passive mode locking have demonstrated, for the following ratio between the values T_2 and T_{rt} :

$$T_2 \ll T_{rt},$$

the laser naturally tends to operate in the standard (incoherent) passive mode-locking regime so that the duration τ_p of the produced mode-locked pulse obeys the inequalities:

$$T_2 \ll \tau_p \ll T_{rt}.$$

In the opposite case of a very short round-trip time:

$$T_{rt} \ll T_2$$

(this case corresponds, for instance, to semiconductor vertical-cavity surface-emitting lasers) the pulsed dynamical regime with $\tau_p < T_{rt}$ cannot set in, since the medium relaxation is negligibly small over the round-trip time and thus cannot promote the onset of the mode locking. Instead, the laser in this case is to operate in the single-longitudinal mode regime with the characteristic time \tilde{T} :

$$T_{rt} \ll T_2 \ll \tilde{T}.$$

Thus we are mainly interested in the following parameter range for the phase relaxation time T_2 :

$$T_2 \sim T_{rt}. \quad (19)$$

In this case it is reasonable to expect the onset of the coherent mode-locking regime with the pulse duration τ_p :

$$\tau_p \ll T_2 \sim T_{rt},$$

so that the pulse indeed coherently interacts with the intracavity medium.

III. DYNAMICS OF A TWO-SECTION RING-CAVITY LASER

Having derived the model Eq. (10) for coherent mode locking, we proceed with applying this model to analyze the

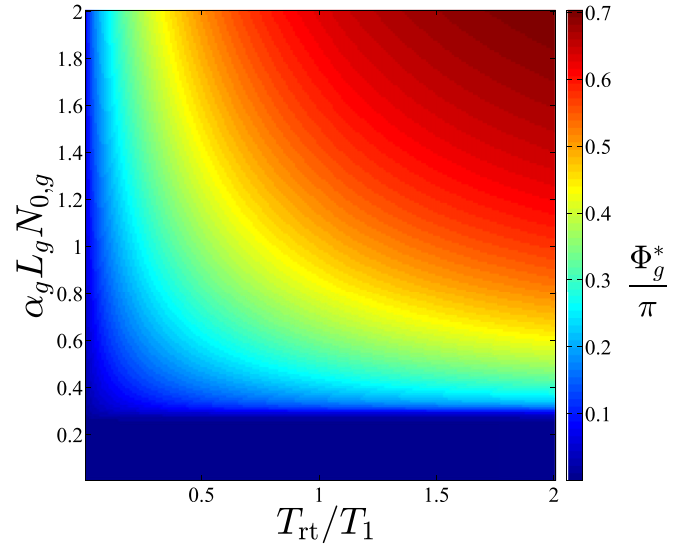


FIG. 2. The steady-state solution for the pulse area Φ^* at the end of the gain section $\Phi_g(L_{\text{gain}})$ vs the parameters T_{rt}/T_1 and $\alpha_g L_g N_{0,g}$; other parameters are $r = 0.95$, $m_d = 1$, $T_{rt}/T_2 = 1$, and $\alpha_a L_a N_{0,a} = -0.8\alpha_g L_g N_{0,g}$.

possible dynamical regimes in such lasers. In our treatment we consider a two-section ring cavity with the unidirectional field propagation, as schematically illustrated in Fig. 1. All mirrors are assumed fully reflecting, except for the output mirror M possessing the amplitude reflection coefficient $r = r(\omega_{12})$ at the pulse carrier frequency ω_{12} . The unidirectional field propagation in the cavity can be ensured, e.g., by placing a respective optical switch into the cavity.

First we examine the case of identical media both in the gain and absorber sections, what implies $m_d = 1$, $T_{1,g} = T_{1,a} = T_1$, and $T_{2,g} = T_{2,a} = T_2$. The control parameters to be varied in this case include the dimensionless values $\alpha_a L_a N_{0,a}$, $\alpha_g L_g N_{0,g}$, T_{rt}/T_1 , T_{rt}/T_2 , and r . We solve the first equation in the system Eq. (10) using the fourth-order Runge-Kutta method.

Figure 2 shows the steady values of the pulse area Φ^* at the output of the gain section, as the parameters T_{rt}/T_1 and $\alpha_g L_g N_{0,g}$ are varied. The absorption rate in the absorber section is fixed here according to the relation $\alpha_a L_a N_{0,a} = -0.8\alpha_g L_g N_{0,g}$ to meet the lasing criteria Eq. (18).

In the whole considered range of the pulse parameters the laser rapidly approaches a stable steady regime with the constant values of both the pulse area at the end of both laser sections and the constant values of the medium quantities at each round trip in the cavity. A respective example is shown in Fig. 3, where the evolution of the pulse area and the medium quantities is plotted as the functions of the number of round trips in the cavity. Initially both media were taken in the equilibrium state with no induced polarization, fully ground-state population in the absorber $N_{0,a} = -N_0$, and fully inverted population in the gain $N_{0,g} = N_0$. The initial value of the pulse area at the entrance of the absorber section at the first round trip was taken $\Phi_0 = 0.001\pi$. One can see that the system afterwards evolves towards the steady state and actually reaches it after ≈ 50 round trips in the cavity. Similar behavior

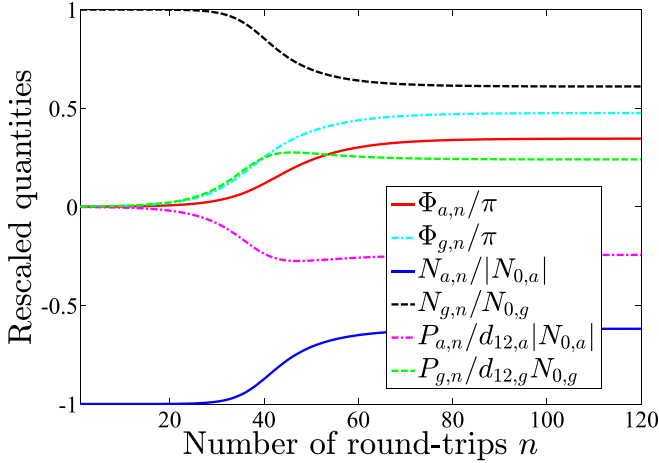


FIG. 3. The evolution of the pulse area at the end of the absorber Φ_a and at the end of the gain Φ_g vs the number of round trips in the cavity n together with the respective values of the medium polarization P_a, P_g and the population inversion N_a, N_g ; the parameters are $r = 0.95$, $m_d = 1$, $T_{rt}/T_1 = 1$, $T_{rt}/T_2 = 1$, $\alpha_g L_g N_{0,g} = 1$, and $\alpha_a L_a N_{0,a} = -0.8$. The initial values of the pulse area $\Phi_0 = 0.001\pi$.

of the temporal evolution of the medium quantities and the pulse area, as the one depicted in Fig. 3, is also obtained for any other values of the control parameters in Fig. 2.

As the gain level and the ratios T_{rt}/T_1 , T_{rt}/T_2 increase, the stable value of the pulse area tends towards π : $\Phi^* \rightarrow \pi$. This finding is in agreement with the result of the paper Ref. [23], where the same was obtained in the limit $T_{rt} \gg T_1, T_2$. However, in the range $T_{rt}/T_2 \sim 1$, the pulse area stays well below π due to the slow medium relaxation, as can be seen in Fig. 2. It should be noted that the value of $\Phi^* = \pi$ corresponds to the stable value of the pulse area in the gain section only. At the same time the stable value of the pulse area in the absorber would be either 0 or 2π . Thus the shaping actions of both media in this case oppose each other, but due to the larger gain rate caused by the condition Eq. (18) in the resulting steady-state laser operation the stable pulse area value still approaches the one for the gain medium $\Phi^* \rightarrow \pi$.

In Fig. 4 we depict a similar diagram for the steady values of the pulse area Φ^* at the output of the gain section but now with the parameters T_{rt}/T_1 and T_{rt}/T_2 varied. One can see that the ratio T_{rt}/T_2 turns out to also have pronounced effect on the stable value Φ^* .

Next, we move on to the case of different media in both laser sections. At the same time it is assumed that the resonant frequencies in the gain and absorber media coincide or at least are close enough to each other. Then we can still use the generalized area theorem Eq. (10) but with different medium parameters in both sections.

We start here with the case where the ratio of the transition dipole moments in the absorber and gain media equals 2: $m_d = 2$. For simplicity, we first suppose equal values of the relaxation variables $T_{1,g} = T_{1,a} = T_1$, $T_{2,g} = T_{2,a} = T_2$. The laser layout with the transition dipole moments in the absorber being twice larger than in the gain is the most preferable one and was mainly considered in most earlier studies of the coherent mode-locking phenomena [13–22]. The reason for it

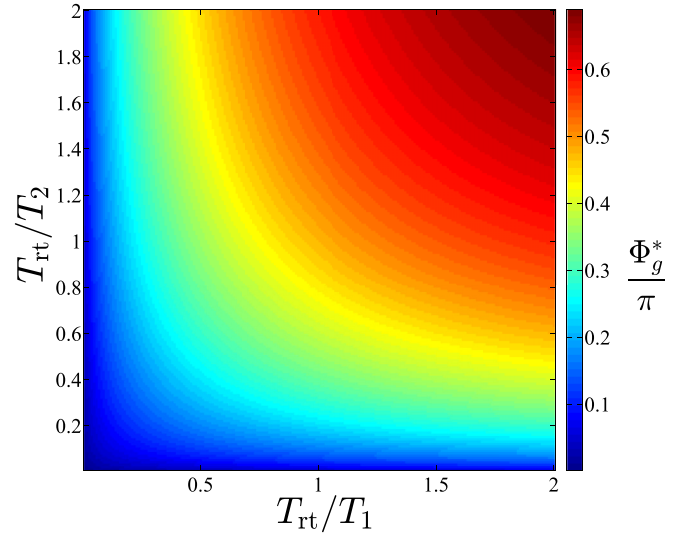


FIG. 4. The steady-state solution for the pulse area Φ^* at the end of the gain section vs the parameters T_{rt}/T_1 and T_{rt}/T_2 ; other parameters are $r = 0.95$, $m_d = 1$, $\alpha_g L_g N_{0,g} = 1$, and $\alpha_a L_a N_{0,a} = -0.8$.

is that for such specific value of the ratio $m_d = d_{12,a}/d_{12,g} = 2$ the stable π pulse in the gain medium at the same time represents the stable 2π pulse in the absorber medium. As the result, the separate action of each of laser media drives the pulse area to the same steady value. In contrast, for other values of the ratio $m_d = d_{12,a}/d_{12,g} \neq 2$ the stable values of the pulse area in each medium separately would be different, so that the system tends to the steady regime, when the actions of both media balance each other.

Figure 5 demonstrates the dependence of the steady values of the pulse area Φ_a^* at the output of the absorber section vs the parameters T_{rt}/T_1 and $\alpha_g L_g N_{0,g}$, similarly to the diagram in Fig. 2 for the ratio $m_d = 1$. The relation between the gain

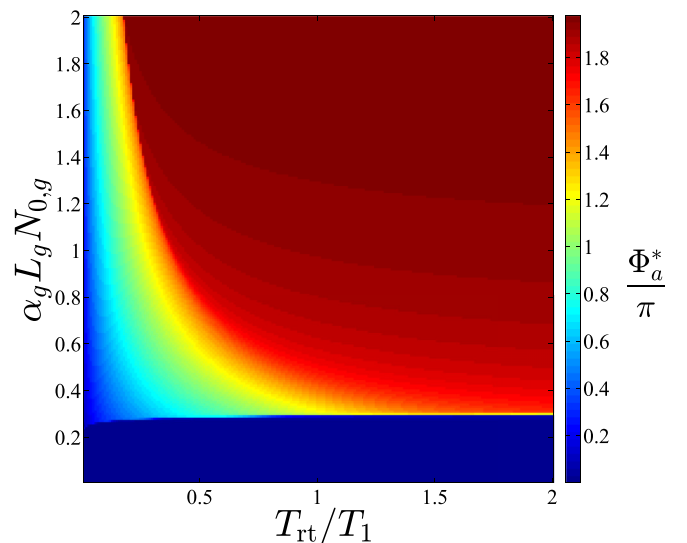


FIG. 5. The steady-state solution for the pulse area Φ_a^* at the end of the absorber section vs the parameters T_{rt}/T_1 and $\alpha_g L_g N_{0,g}$; other parameters are $r = 0.95$, $m_d = 2$, $T_{rt}/T_2 = 1$, and $\alpha_a L_a N_{0,a} = -0.8\alpha_g L_g N_{0,g}$.

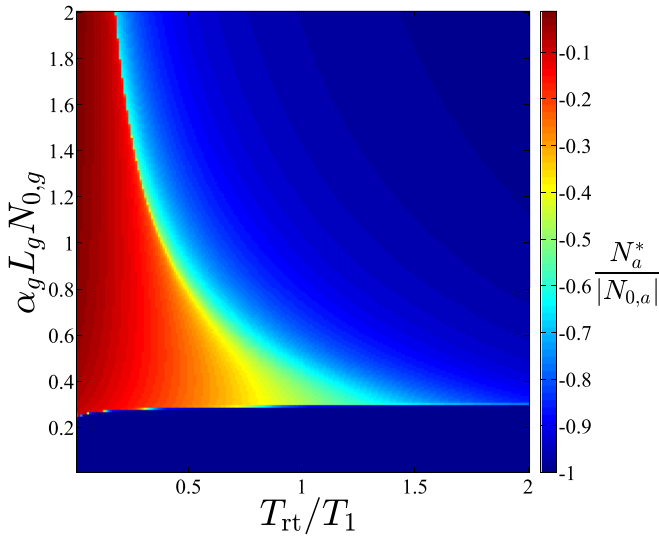


FIG. 6. The steady-state solution for the population inversion N_a^* in the absorber section vs the parameters T_{rt}/T_1 and $\alpha_g L_g N_{0,g}$; other parameters are $r = 0.95$, $m_d = 2$, $T_{rt}/T_2 = 1$, and $\alpha_a L_a N_{0,a} = -0.8\alpha_g L_g N_{0,g}$.

and absorption rates in both laser sections is again taken as $\alpha_a L_a N_{0,a} = -0.8\alpha_g L_g N_{0,g}$ in order to meet the lasing condition [Eq. (18)].

As it could be intuitively expected from the above, the stable value of the pulse area at the output of the absorber section Φ_a^* is to go to 2π , with the corresponding value at the output of the gain section Φ_g^* tending to π . As can be seen from the diagram in Fig. 5, the system indeed approaches this values as long as the gain rate sufficiently exceeds the lasing threshold Eq. (18) and the population inversion recovery is not too slow, namely at least $T_{rt}/T_1 \approx 1$. When the gain level is close to the lasing threshold and the population inversion recovery is relatively slow, namely the ratio T_{rt}/T_1 is well below 1, the steady values of the pulse area constitute just a fraction of the values $\Phi_g^* = \pi$, $\Phi_a^* = 2\pi$.

In Fig. 6 the steady-state values of the population inversion in the absorber section are plotted for the parameters from Fig. 5. In accordance with Fig. 5, for the pumping rate well above the lasing threshold and for the fast recovery of the population inversion the stable value of the absorber population tends to its initial value $N_{0,a}$, since, as discussed above, the pulse propagation in the absorber section in this case approaches the 2π -pulse dynamics. In the case of very slow inversion recovery, i.e., $T_{rt} \ll T_1$, as can be seen in Fig. 6, the stable value of the population inversion goes to zero regardless of the pumping rate. The respective steady value of the pulse area in this limit in Fig. 5 goes well below π . Thus, with so slow absorption recovery the laser system only manages to support the temporal variations of the population inversion nearby the zero value.

At the same time the dependence of the steady-state values of the population inversion in the gain section on the same control parameters exhibits significant differences. The analogous diagram for the gain medium is plotted in Fig. 7. One can see that in Fig. 7 the steady value of the gain level shows almost no dependence on the pumping level $\alpha_g L_g N_{0,g}$ and is

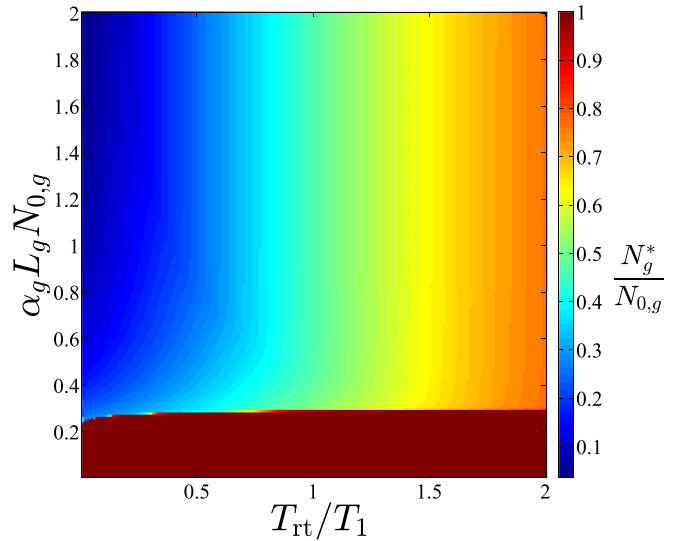


FIG. 7. The steady-state solution for the population inversion N_g^* in the gain section vs the parameters T_{rt}/T_1 and $\alpha_g L_g N_{0,g}$; other parameters are $r = 0.95$, $m_d = 2$, $T_{rt}/T_2 = 1$, and $\alpha_a L_a N_{0,a} = -0.8\alpha_g L_g N_{0,g}$.

primarily determined solely by the inversion recovery time T_1 . The faster this population inversion recovers, the closer the stable gain value comes to the initial pumping level $N_{0,g}$.

Let us now consider another value of the ratio of the transition dipole moments in the absorber and gain media, namely $m_d = 3$. As before, we take for the sake of simplicity the equal values of the relaxation times $T_{1,g} = T_{1,a} = T_1$ and $T_{2,g} = T_{2,a} = T_2$. The choice $m_d = 3$ is not an accidental but is inspired by the specifics of the coherent pulse propagation in accordance with the classical area theorem Eq. (14). As was first noticed in Ref. [51] for the classical area theorem Eq. (14), in order to achieve the pulse compression on its coherent propagation in the absorbing medium, the initial pulse area has to fall into the range $(2\pi; 3\pi)$. For smaller initial pulse area the pulse duration in the absorber would grow. At the same time the pulse compression in the gain naturally occurs for the initial pulse area in the range $(0; \pi)$, as the initial pulse evolves towards π pulse while growing in amplitude and simultaneously getting compressed in duration. In the context of the coherent mode locking in lasers, it means that one could expect to achieve the shortest output mode-locked pulses when choosing the intracavity media to obey the ratio of the dipole moments $m_d = 3$. Indeed, from the above it could be expected that at least within the classical area theorem Eq. (14) the pulse area in the gain would grow to π , while in the absorber it would decline in the range $(2\pi; 3\pi)$. In both sections, therefore, the propagating pulse would experience temporal compression.

The respective dependence of the steady values of the pulse area Φ_a^* at the output of the absorber section on the parameters T_{rt}/T_1 and $\alpha_g L_g N_{0,g}$ is depicted in Fig. 8. Again, we fixed the gain and absorption rates in both laser sections as $\alpha_a L_a N_{0,a} = -0.8\alpha_g L_g N_{0,g}$. One can see that if the inversion recovery is not too slow, then the pulse area indeed attains the steady values in the range $(2\pi; 3\pi)$. The analogous diagram for the pulse area

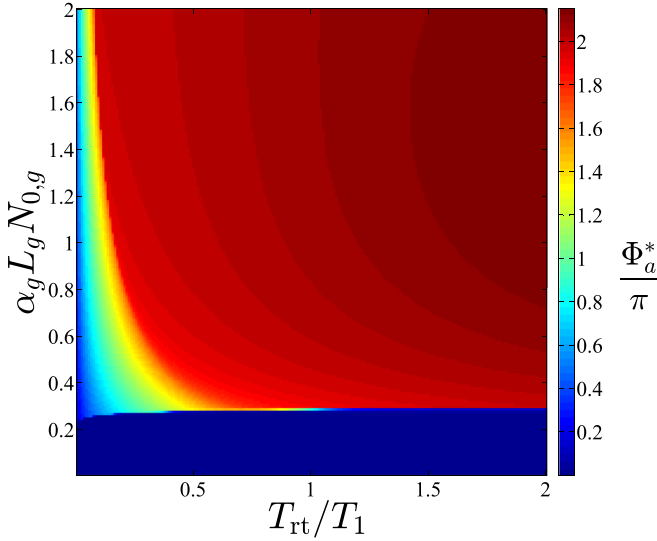


FIG. 8. The steady-state solution for the pulse area Φ_a^* at the end of the absorber section vs the parameters T_{rt}/T_1 and $\alpha_g L_g N_{0,g}$; other parameters are $r = 0.95$, $m_d = 3$, $T_{rt}/T_2 = 1$, and $\alpha_a L_a N_{0,a} = -0.8\alpha_g L_g N_{0,g}$.

Φ_g^* at the output of the gain section is provided in Fig. 9. Here the pulse area tends to the stable value equal to π . The overall view of Fig. 9 appears qualitatively similar to the diagram for Φ_g^* in Fig. 2 for the ratio $m_d = 1$. At the same time one can see that, as the pumping rate $N_{0,g}$ exceeds the lasing threshold, the steady values of the Φ_g^* in Fig. 9 approach π much faster, as compared to Fig. 2. The reason for that is the contribution of the absorber, namely, while for $m_d = 1$ the pulse area in the absorber goes to 0, for $m_d = 3$ the stable value of the pulse area in the absorber alone would be 2π , what yields $2\pi/3$ after rescaling to the gain medium parameters according to Eq. (12) (as the transition dipole moments differ by the factor

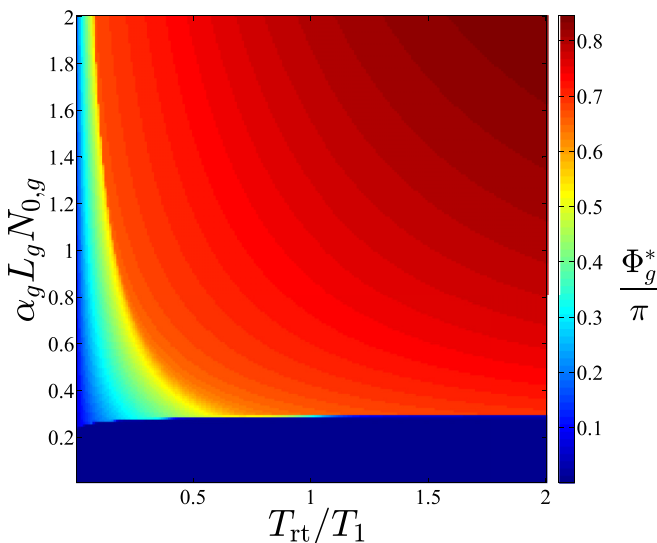


FIG. 9. The steady-state solution for the pulse area Φ_g^* at the end of the gain section vs the parameters T_{rt}/T_1 and $\alpha_g L_g N_{0,g}$; other parameters are $r = 0.95$, $m_d = 3$, $T_{rt}/T_2 = 1$, and $\alpha_a L_a N_{0,a} = -0.8\alpha_g L_g N_{0,g}$.

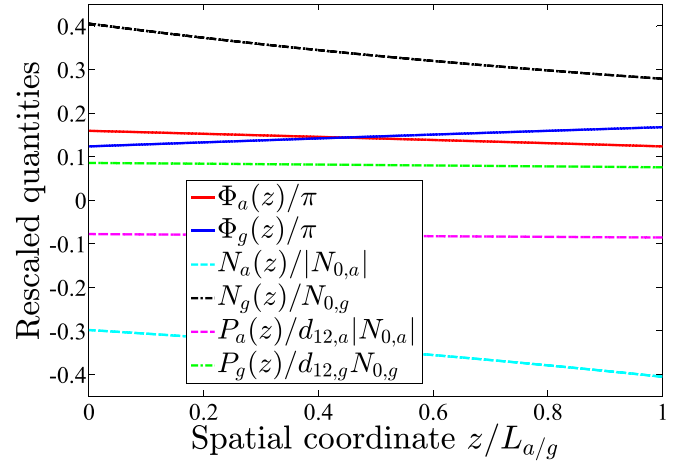


FIG. 10. The spatially varying solutions for the pulse area $\Phi_a(z)$, $\Phi_g(z)$ and the medium polarization $P_a(z)$, $P_g(z)$ and the population inversion $N_a(z)$, $N_g(z)$ in both laser sections in the steady operation regime; the parameters are $r = 0.95$, $m_d = 1$, $T_{rt}/T_1 = 0.1$, $T_{rt}/T_2 = 1$, $\alpha_g L_g N_{0,g} = 1$, and $\alpha_a L_a N_{0,a} = -0.8$.

of $m_d = 3$). As the result, the steady values of Φ_g^* get close to π for much smaller pumping levels.

Let us now take a closer look at the spatial extension of the pulse area and the medium quantities. We proceed therefore with the analysis of the spatially extended solutions of Eq. (10). Figure 10 shows examples of the obtained spatially extended solutions for the parameters $m_d = 1$, $T_{rt}/T_1 = 0.1$. The functions for the absorber section are displayed vs the rescaled coordinate z/L_a and the functions for the gain section are plotted vs the rescaled coordinate z/L_g . The laser system in this case turns out to rapidly evolve towards the steady distributions from Fig. 10. As can be seen in Fig. 10, the pulse area in the steady regime monotonously grows in the gain medium towards π and monotonously decreases in the absorber medium, similarly to the dynamics predicted within the classical area theorem [51]. Still the achieved values of the pulse area even in the gain in Fig. 10 is just a small fraction of π due to the slow inversion relaxation.

Figure 11 illustrates the spatially extended solutions for $m_d = 1$ and much faster relaxation of the inverted population $T_{rt}/T_1 = 1$, i.e., the parameters of Fig. 3. As Fig. 3 shows the laser system in this case rapidly reaches the steady regime. The performed solution with the spatial distribution has led to the same result. The resulting steady spatial solutions in Fig. 10 perfectly match those from Fig. 3. Because of the increased recovery rate of the gain as compared to Fig. 10, the steady values of the pulse area appear to be much closer to π . In general, our numerical studies have shown that further increasing the value T_{rt}/T_1 leads to the pulse area values approaching π , in full agreement to the diagram in Fig. 2.

In Fig. 12 the similar steady spatially extended solutions are demonstrated for the same parameters as in Fig. 10, except for the ratio m_d increased to $m_d = 2$. For this ratio the stable area values in both media should in fact coincide, as $\Phi_g = \pi$ simultaneously means $\Phi_a = 2\pi$. However, due to the slow gain recovery during the round-trip time $T_{rt}/T_1 = 0.1$ the pulse area in the gain section does not get over even the

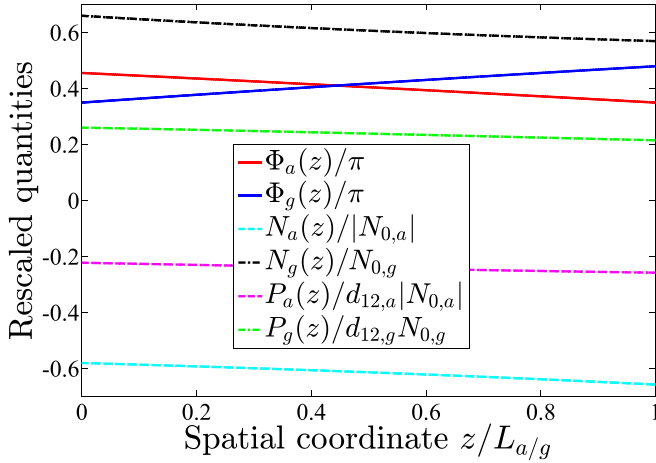


FIG. 11. The spatially varying solutions for the pulse area $\Phi_a(z)$, $\Phi_g(z)$ and the medium polarization $P_a(z)$, $P_g(z)$ and the population inversion $N_a(z)$, $N_g(z)$ in both laser sections in the steady operation regime; the parameters are $r = 0.95$, $m_d = 1$, $T_{\text{rt}}/T_1 = 1$, $T_{\text{rt}}/T_2 = 1$, $\alpha_g L_g N_{0,g} = 1$, and $\alpha_a L_a N_{0,a} = -0.8$.

value $\pi/2$. Hence, the respective pulse area in the absorber is below π and decreases on propagation similar to what is predicted by the classical area theorem [51].

If the gain recovery during the round-trip time gets increased to the value $T_{\text{rt}}/T_1 = 1$, then the situation changes. Now the gain level in the steady operation regime turns out to be sufficient to assure the pulse area to reach π in the gain section. The respective simulation results are plotted in Fig. 13. At the same time, as this pulse enters the absorber section, its pulse area calculated through the transition dipole moment of the absorber with Eq. (1) almost equals the stable value 2π . This leads in fact to very fast convergence of all spatially varying functions to the steady ones in Fig. 13.

Finally, Fig. 14 shows the spatially varying solutions in the steady regime with the ratio of the dipole moments

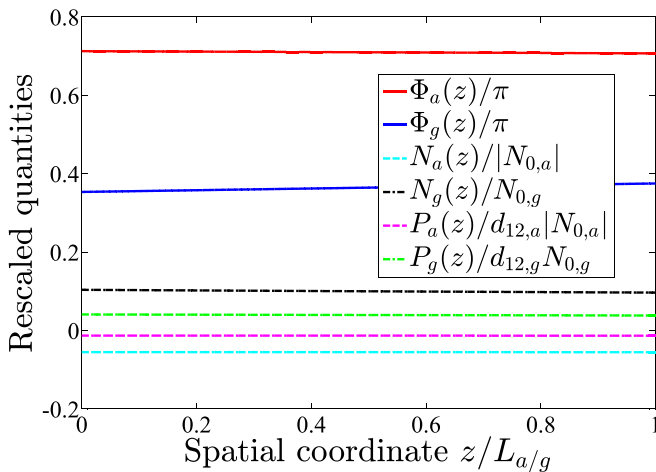


FIG. 12. The spatially varying solutions for the pulse area $\Phi_a(z)$, $\Phi_g(z)$ and the medium polarization $P_a(z)$, $P_g(z)$ and the population inversion $N_a(z)$, $N_g(z)$ in both laser sections in the steady operation regime; the parameters are $r = 0.95$, $m_d = 2$, $T_{\text{rt}}/T_1 = 0.1$, $T_{\text{rt}}/T_2 = 1$, $\alpha_g L_g N_{0,g} = 1$, and $\alpha_a L_a N_{0,a} = -0.8$.

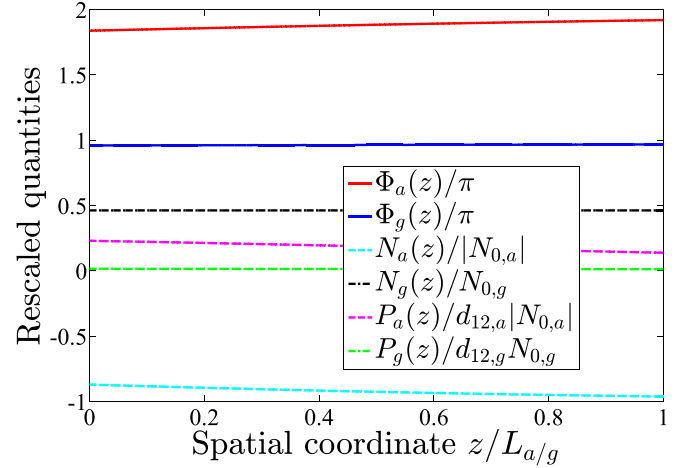


FIG. 13. The spatially varying solutions for the pulse area $\Phi_a(z)$, $\Phi_g(z)$ and the medium polarization $P_a(z)$, $P_g(z)$ and the population inversion $N_a(z)$, $N_g(z)$ in both laser sections in the steady operation regime; the parameters are $r = 0.95$, $m_d = 2$, $T_{\text{rt}}/T_1 = 1$, $T_{\text{rt}}/T_2 = 1$, $\alpha_g L_g N_{0,g} = 1$, and $\alpha_a L_a N_{0,a} = -0.8$.

$m_d = 3$ and the slow gain recovery $T_{\text{rt}}/T_1 = 0.1$. Here the slow-enough gain recovery again results in the steady pulse area in the gain medium well below π . Specifically, the largest pulse area at the end of the gain section is below $2\pi/3r$, so when this pulse enters afterwards the absorber section, its pulse area calculated through the transition dipole moment of the absorber with Eq. (1) appears below 2π . As a result, we get the monotonously growing pulse area in the absorber towards 2π , as can be seen in Fig. 14. Since the steady pulse area grows in both laser sections, the convergence to this steady operation happens significantly faster than it would be with enhanced gain recovery.

With increasing the gain recovery rate to $T_{\text{rt}}/T_1 = 1$, the steady value of the pulse area in the gain becomes close to π , as shown in Fig. 15. As the result in the absorber section the

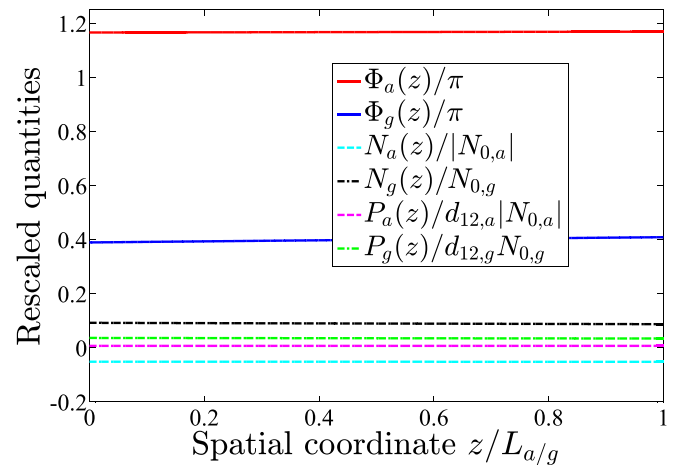


FIG. 14. The spatially varying solutions for the pulse area $\Phi_a(z)$, $\Phi_g(z)$ and the medium polarization $P_a(z)$, $P_g(z)$ and the population inversion $N_a(z)$, $N_g(z)$ in both laser sections in the steady operation regime; the parameters are $r = 0.95$, $m_d = 3$, $T_{\text{rt}}/T_1 = 0.1$, $T_{\text{rt}}/T_2 = 1$, $\alpha_g L_g N_{0,g} = 1$, and $\alpha_a L_a N_{0,a} = -0.8$.

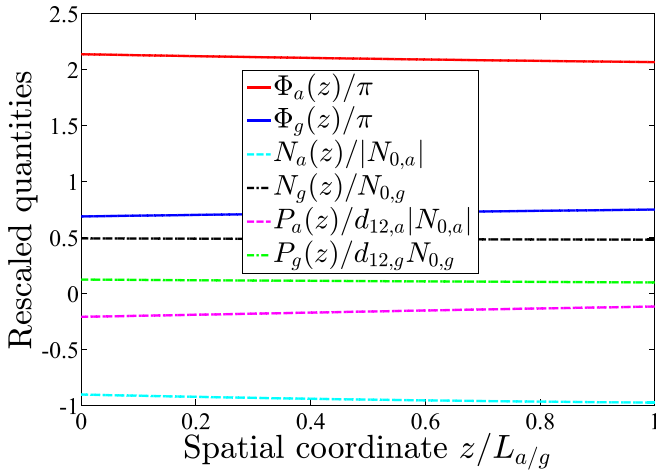


FIG. 15. The spatially varying solutions for the pulse area $\Phi_a(z)$, $\Phi_g(z)$ and the medium polarization $P_a(z)$, $P_g(z)$ and the population inversion $N_a(z)$, $N_g(z)$ in both laser sections in the steady operation regime; the parameters are $r = 0.95$, $m_d = 3$, $T_{rt}/T_1 = 1$, $T_{rt}/T_2 = 1$, $\alpha_g L_g N_{0,g} = 1$, and $\alpha_a L_a N_{0,a} = -0.8$.

pulse area decreases in the range $(2\pi; 3\pi)$ towards the stable value 2π .

Last, we consider the case of unequal and strongly differing relaxation times T_1 in the gain and absorber media. To be specific, we take the case of a slow absorber having the absorption recovery rate $T_{1,a}$ several orders of magnitude larger than the gain recovery rate $T_{1,g}$. As the result, in this case the absorption rate makes it to recover to a much lower value than in the case of the fast absorber. Hence, the contribution of the absorber section to the shaping of the produced mode-locked pulse is reduced, while the role of the gain section becomes the major.

As our numerical simulations demonstrate, the resulting dynamics when taking such a slow absorber does not undergo any qualitative differences. Still the exact values of the achieved pulse area in the steady lasing regime are altered and get closer to their stable values in the gain section. This effect is especially pronounced when the stable pulse areas in both sections differ, like for $m = 1$ above. The corresponding diagram is plotted in Fig. 16 for the pulse area at the end of the gain section for $m = 1$ and a slow absorber with $T_{1,a} = 100 T_{1,g}$. From the comparison of Figs. 2 and 16 one can indeed see that with a slow absorber the pulse area in the gain medium much faster reaches the π value due to the major role of the gain section in the mode-locking dynamics in this case. Similar reasoning holds also, e.g., for the m values nearby $m = 3$. Inversely, if $m = 2$, so that the stable values of the pulse area in both sections coincide, a slow absorber leads to the slower convergence to that stable value, since instead of the joint action of both laser sections just the gain section mainly contributes now.

In summary, the proposed approach possesses some natural limitations. Specifically, it solely deals with the pulse area Eq. (1) to describe the dynamics of the electric field inside the laser cavity. At the same time the electric field strength $E(z, t)$ appears to be completely inaccessible within the framework of the developed model. As the result, one cannot explicitly

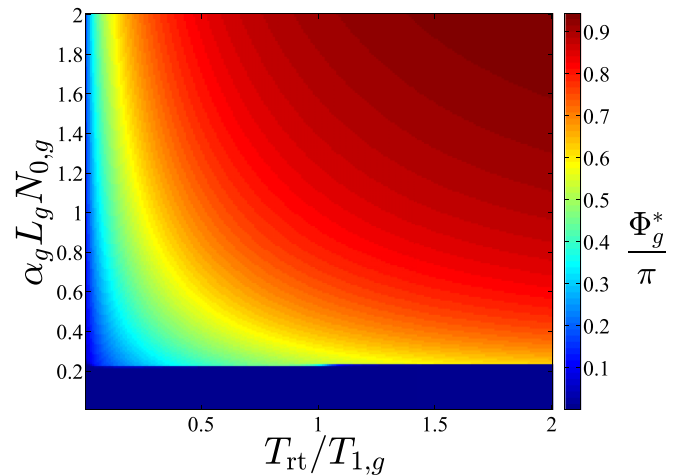


FIG. 16. The steady-state solution for the pulse area Φ_g^* at the end of the gain section $\Phi_g(L_{\text{gain}})$ vs the parameters T_{rt}/T_1 and $\alpha_g L_g N_{0,g}$ in the case of a slow absorber: $T_{1,a} = 100 T_{1,g}$; other parameters are $r = 0.95$, $m_d = 1$, $T_{rt}/T_2 = 1$, and $\alpha_a L_a N_{0,a} = -0.8 \alpha_g L_g N_{0,g}$.

determine the shape of the generated mode-locked pulses. Similarly, such pulse parameters, as the pulse duration or the pulse amplitude, stay in fact unknown, as being veiled by the value of the pulse area Eq. (1). In order to get these quantities though one would need to run the numerical solution of the full system of Maxwell-Bloch equations for the electric field and the intracavity media.

However, the derived model for coherent mode locking allows to easily study the general properties of the lasing dynamics. In particular, it is able to predict the possible regimes of the laser operation and readily perform their stability analysis. Besides, the parameter dependencies can be easily investigated. This is of special importance as even the above considered two-section laser possesses quite a large number of control parameters, related to the media properties, pumping, and the cavity. Therefore studies of the laser dynamics vs the variation of certain parameters turn out in high demand. Solving the full system of Maxwell-Bloch equations for each parameter set would require huge computational resources, especially when many laser parameters are to be scanned. In contrast, the suggested above model can handle this task in an elegant and utterly simple way.

IV. CONCLUSION

We have come up with a convenient and easy-to-use analytical model for the dynamics of the coherent passive mode locking in two-section lasers with a ring cavity. We would like to note that to the best of our knowledge there have been no analytical tools developed so far for the analysis of the truly coherent pulse propagation in laser cavity setups.

The proposed model relies on the generalized area theorem for the coherent pulse propagation through an arbitrarily pre-excited resonant medium. The obtained model consists of the direct algebraic equations for the induced polarization and the population inversion of both gain and absorber laser media at each spatial point and at each round trip inside the cavity.

These expressions are coupled to an equation for the spatially varying pulse area of the generated pulse $\Phi(z)$.

Remarkably, the evolution equation for the pulse area can either be a first-order differential one, or it can be integrated and put to the integral form. In the latter case we end up with no differential equations at all. As we have demonstrated, it is possible to go even further with simplifying the model, if making an assumption of negligibly varying medium quantities over the entire length of the respective laser sections. As we have shown by solving the model in its general form, such approximation is reasonably justified in almost the whole considered range of laser parameters. On such an assumption, the spatial integrals of the medium quantities get largely reduced, so that we eventually arrive to a set of explicit equations for the pulse area and medium parameters at the next round trip expressed directly through their values at the previous round trip.

We have applied our model to examine in details the spatiotemporal dynamics of a two-section laser in the regime of the coherent mode locking. We have specifically investigated the dependence of the arising stable pulse generation on the parameters of the active media and the laser cavity.

For a ring-cavity two-section laser it was demonstrated that the steady stable regime is always reached in the whole

considered range of the varying parameters, including the medium relaxation times T_1 and T_2 , the pumping rate in the gain section $N_{0,g}$ and the ratio of the transition dipole moments in both media m_d . The last parameter, i.e., the ratio m_d defined by Eq. (13), was found to be of key importance here, as it determines the range of the achievable values of the pulse area $\Phi(z)$ in the arising steady generation.

It is particularly remarkable that the laser system operating in such a coherent mode-locking regime always rapidly evolves towards its stable steady-state lasing. We have not actually been able to find any instabilities in the derived model as well as any periodic or other oscillating solutions. These findings therefore could be indicative of the superior reliability of coherently mode-locked lasers. Hence, in our view the paper findings can promote the pursuit of the creation of ultracompact laser sources of ultrashort pulses where the coherent effects are to play the key role in the lasing onset.

ACKNOWLEDGMENTS

The authors acknowledge support from the Foundation for the Advancement of Theoretical Physics and Mathematics “BASIS.” The numerical simulations were in part supported by the Russian Science Foundation, Project No. 21-72-10028.

-
- [1] U. Keller, *Appl. Phys. B* **100**, 15 (2010).
 - [2] Y. Han, Y. Guo, B. Gao, C. Ma, R. Zhang, and H. Zhang, *Prog. Quantum Electron.* **71**, 100264 (2020).
 - [3] U. Keller, *Ultrafast Lasers: A Comprehensive Introduction to Fundamental Principles with Practical Applications* (Springer, Berlin, 2022), pp. 419–546.
 - [4] F. Prati, A. M. Perego, S. Barland, and G. J. De Valcárcel, *Photoniques* **122**, 70 (2023).
 - [5] A. Yadav, N. B. Chichkov, E. A. Avrutin, A. Gorodetsky, and E. U. Rafailov, *Prog. Quantum Electron.* **87**, 100451 (2023).
 - [6] A. H. Quarterman, K. G. Wilcox, V. Apostolopoulos, Z. Mihoubi, S. P. Elsmere, I. Farrer, D. A. Ritchie, and A. Tropper, *Nat. Photon.* **3**, 729 (2009).
 - [7] P. Klopp, U. Griebner, M. Zorn, and M. Weyers, *Appl. Phys. Lett.* **98**, 071103 (2011).
 - [8] M. Gaafar, P. Richter, H. Keskin, C. Möller, M. Wichmann, W. Stolz, A. Rahimi-Iman, and M. Koch, *Opt. Express* **22**, 28390 (2014).
 - [9] I. Kilen, J. Hader, J. V. Moloney, and S. W. Koch, *Optica* **1**, 192 (2014).
 - [10] D. Waldburger, S. M. Link, M. Mangold, C. G. E. Alfieri, E. Gini, M. Golling, B. W. Tilma, and U. Keller, *Optica* **3**, 844 (2016).
 - [11] M. A. Gaafar, A. Rahimi-Iman, K. A. Fedorova, W. Stolz, E. U. Rafailov, and M. Koch, *Adv. Opt. Photon.* **8**, 370 (2016).
 - [12] E. Riccardi, V. Pistore, S. Kang, L. Seitner, A. De Vetter, C. Jirauschek, J. Mangeney, L. Li, A. G. Davies, E. H. Linfield, A. C. Ferrari, S. S. Dhillon, and M. S. Vitiello, *Nat. Photon.* **17**, 607 (2023).
 - [13] V. V. Kozlov, *Phys. Rev. A* **56**, 1607 (1997).
 - [14] C. R. Menyuk and M. A. Talukder, *Phys. Rev. Lett.* **102**, 023903 (2009).
 - [15] M. A. Talukder and C. R. Menyuk, *Phys. Rev. A* **79**, 063841 (2009).
 - [16] V. V. Kozlov, N. N. Rosanov, and S. Wabnitz, *Phys. Rev. A* **84**, 053810 (2011).
 - [17] V. V. Kozlov and N. N. Rosanov, *Phys. Rev. A* **87**, 043836 (2013).
 - [18] R. Arkhipov, M. Arkhipov, and I. Babushkin, *Opt. Commun.* **361**, 73 (2016).
 - [19] R. M. Arkhipov, M. V. Arkhipov, I. Babushkin, and N. N. Rosanov, *Opt. Lett.* **41**, 737 (2016).
 - [20] R. M. Arkhipov, A. V. Pakhomov, M. V. Arkhipov, I. V. Babushkin, and N. N. Rosanov, *Sci. Rep.* **11**, 1147 (2021).
 - [21] R. Arkhipov, M. Arkhipov, A. Pakhomov, I. Babushkin, and N. N. Rosanov, *Phys. Rev. A* **105**, 013526 (2022).
 - [22] A. Outafat, S. Faci, E. Richalot, S. Protat, and C. Algani, *Opt. Quant. Electron.* **54**, 283 (2022).
 - [23] A. Pakhomov, M. Arkhipov, N. Rosanov, and R. Arkhipov, *Phys. Rev. A* **107**, 013510 (2023).
 - [24] M. Arkhipov, A. Shimko, R. Arkhipov, I. Babushkin, A. Kalinichev, A. Demircan, U. Morgner, and N. Rosanov, *Laser Phys. Lett.* **15**, 075003 (2018).
 - [25] M. V. Arkhipov, A. A. Shimko, N. N. Rosanov, I. Babushkin, and R. M. Arkhipov, *Phys. Rev. A* **101**, 013803 (2020).
 - [26] P. Borri, W. Langbein, S. Schneider, U. Woggon, R. L. Sellin, D. Ouyang, and D. Bimberg, *Phys. Rev. B* **66**, 081306(R) (2002).
 - [27] E. Beham, A. Zrenner, F. Findeis, M. Bichler, and G. Abstreiter, *Phys. Status Solidi B* **238**, 366 (2003).
 - [28] H. Choi, V.-M. Gkortsas, L. Diehl, D. Bour, S. Corzine, J. Zhu, G. Hoefler, F. Capasso, F. Kärtner, and T. Norris, *Nat. Photon.* **4**, 706 (2010).
 - [29] O. Karni, A. Capua, G. Eisenstein, V. Sichkovskiy, V. Ivanov, and J. P. Reithmaier, *Opt. Express* **21**, 26786 (2013).

- [30] M. Kolarczik, N. Owschimikow, J. Korn, B. Lingnau, Y. Kaptan, D. Bimberg, E. Schöll, K. Lüdge, and U. Woggon, *Nat. Commun.* **4**, 2953 (2013).
- [31] S. Nandi, E. Olofsson, M. Bertolino, S. Carlström, F. Zapata, D. Busto, C. Callegari, M. Di Fraia, P. Eng-Johnsson, R. Feifel, G. Gallician, M. Gisselbrecht, S. Maclot, L. Neoričić, J. Peschel, O. Plekan, K. Prince, R. Squibb, S. Zhong, and J. Dahlström, *Nature (Lond.)* **608**, 488 (2022).
- [32] J. Harvey, J. Dudley, P. Curley, C. Spielmann, and F. Krausz, *Opt. Lett.* **19**, 972 (1994).
- [33] J. Dudley, J. Harvey, and R. Leonhardt, *J. Opt. Soc. Am. B* **10**, 840 (1993).
- [34] J. Dudley and J. Harvey, *Opt. Commun.* **82**, 517 (1991).
- [35] H. Haus, *IEEE J. Quant. Electron.* **11**, 736 (1975).
- [36] H. A. Haus, *IEEE J. Sel. Top. Quant. Electron.* **6**, 1173 (2000).
- [37] G. New, *IEEE J. Quant. Electron.* **10**, 115 (1974).
- [38] F. Kartner, I. Jung, and U. Keller, *IEEE J. Sel. Top. Quant. Electron.* **2**, 540 (1996).
- [39] R. Paschotta and U. Keller, *Appl. Phys. B* **73**, 653 (2001).
- [40] A. G. Vladimirov and D. Turaev, *Phys. Rev. A* **72**, 033808 (2005).
- [41] J. Hausen, K. Lüdge, S. V. Gurevich, and J. Javaloyes, *Opt. Lett.* **45**, 6210 (2020).
- [42] M. Nizette and A. G. Vladimirov, *Phys. Rev. E* **104**, 014215 (2021).
- [43] M. Rossetti, P. Bardella, and I. Montrosset, *IEEE J. Quant. Electron.* **47**, 569 (2011).
- [44] J. Hausen, S. Meinecke, B. Lingnau, and K. Lüdge, *Phys. Rev. Appl.* **11**, 044055 (2019).
- [45] A. G. Vladimirov, S. Suchkov, G. Huyet, and S. K. Turitsyn, *Phys. Rev. A* **104**, 033525 (2021).
- [46] S. Meinecke and K. Lüdge, *Phys. Rev. Appl.* **18**, 064070 (2022).
- [47] A. M. Perego, B. Garbin, F. Gustave, S. Barland, F. Prati, and G. J. De Valcárcel, *Nat. Commun.* **11**, 311 (2020).
- [48] F. Prati, A. Perego, J. Redondo, and G. de Valcarcel, *EPJ Web Conf.* **287**, 08013 (2023).
- [49] S. L. McCall and E. L. Hahn, *Phys. Rev. Lett.* **18**, 908 (1967).
- [50] S. L. McCall and E. L. Hahn, *Phys. Rev.* **183**, 457 (1969).
- [51] L. Allen and J. H. Eberly, *Optical Resonance and Two-level Atoms* (Wiley, New York, 1975).
- [52] J. Eberly, *Opt. Express* **2**, 173 (1998).
- [53] S. Hughes, *Phys. Rev. Lett.* **81**, 3363 (1998).
- [54] O. D. Mücke, T. Tritschler, M. Wegener, U. Morgner, and F. X. Kärtner, *Phys. Rev. Lett.* **87**, 057401 (2001).
- [55] T. Chanelière, *Opt. Express* **22**, 4423 (2014).
- [56] S. Moiseev and R. Urmancheev, [arXiv:2301.10294](https://arxiv.org/abs/2301.10294).
- [57] S. Moiseev and R. Urmancheev, *Opt. Lett.* **47**, 3812 (2022).
- [58] S. A. Moiseev, M. Sabooni, and R. V. Urmancheev, *Phys. Rev. Res.* **2**, 012026(R) (2020).
- [59] S. A. Moiseev, M. M. Minnegaliev, E. S. Moiseev, K. I. Gerasimov, A. V. Pavlov, T. A. Rupasov, N. N. Skryabin, A. A. Kalinkin, and S. P. Kulik, *Phys. Rev. A* **107**, 043708 (2023).
- [60] A. Pakhomov, M. Arkhipov, N. Rosanov, and R. Arkhipov, *Phys. Rev. A* **108**, 023506 (2023).